Journal of Solid Mechanics Vol. 9, No. 4 (2017) pp. 865-877

An Investigation of Stress and Deformation States of Rotating Thick Truncated Conical Shells of Functionally Graded Material

A.K. Thawait [1, *], L. Sondhi [2], Sh. Bhowmick [3], Sh. Sanyal [3]

[1]*Department of Mechanical Engineering, Institute of Technology, Guru Ghasidas Vishwavidyalaya, Bilaspur, 495009, India*
[2]*Department of Mechanical Engineering, Shri Shankaracharya Technical Campus, SSGI, Bhilai, 490020, India*
[3]*Department of Mechanical Engineering, National Institute of Technology (NIT), Raipur, 492010, India*

Received 3 August 2017; accepted 7 October 2017

ABSTRACT

The present study aims at investigating stress and deformation behavior of rotating thick truncated conical shells subjected to variable internal pressure. Material prpperties of the shells are graded along the axial direction by Mori-tanaka scheme, which is achieved by elemental gradation of the properties.Governing equations are derived using principle of stsionary total potential (PSTP) and shells are subjected to clamped- clamped boundary conditions. Aluminum-zirconia, metal-ceramic and ceramic-metal FGM is considered and effects of grading index of material properties and pressure distribution are analyzed. Distribution of Radial displacement and circumferential stress in both radial and axial direction is presented. Further a comparison of behaviors of different FGM shells and homogeneous shells are made which shows, a significant reduction in stresses and deformations of FGM shells as compared to homogeneous shell. FGM shell having value of grading parameter $n = 2$ is most suitable for the purpose of rotating conical shells having variable pressure distribution as compared to homogeneous shell and shell having other values of grading parameter n.

Keywords : Rotating thick truncated conical shell; Functionally graded material; Linear elastic analysis.

1 INTRODUCTION

FUNCTIONALLY graded materials (FGMs) are multi phase composite materials that have continuous and smooth spatial variations of physical and mechanical properties. The gradation of material properties in FGMs is achieved by continuously varying the volume fractions of the constituents. Functionally graded conical shells are widely used in space vehicles, aircrafts, nuclear power plants and many other engineering applications. Asemi et al. [1] have applied Rayleigh–Ritz energy formulation to obtain the elastic behavior of functionally graded thick truncated cone by finite element method. Civalek [3] developed the discrete singular convolution (DSC) algorithm for determining the frequencies of the free vibration of laminated conical shells by using a numerical solution of the governing differential equations of motion based on Love's first approximation thin shell theory. Civalek et al. [4] proposed discrete singular convolution (DSC) method for numerical solution of vibration problem based on Love's

*Corresponding author. Tel.: +91 8103180085.
E-mail address: amkthawait@gmail.com (A.K.Thawait).

first approximation shell theory considering the effects of initial hoop tension and centrifugal and Coriolis accelerations due to rotation. Heydarpour et al. [5] employed The generalized coupled thermoelasticity based on the Lord–Shulman (L-S) theory to study the transient thermoelastic behavior of rotating functionally graded (FG) truncated conical shells subjected to thermal shock with different boundary conditions. Hua [6] made a study of the influences of orthotropic properties and boundary conditions on the free vibrations of a rotating, truncated, circular orthotropic conical shell considering the effects of the Coriolis and centrifugal accelerations and the initial hoop tension based on the Love first-approximation theory and Galerkin procedure. Ma et al. [7] presented a free and forced vibration analysis of coupled conical–cylindrical shells with arbitrary boundary conditions using a modified Fourier–Ritz method. Malekzadeh et al. [8] studied the dynamic behavior of functionally graded (FG) truncated conical shells subjected to asymmetric internal ring-shaped moving loads. The material properties are assumed to have continuous variations in the shell thickness direction and the equations of motion are derived based on the first-order shear deformation theory (FSDT) using Hamilton′s principle. Nejad et al.[9-11] have performed a semi analytical approach using first-order shear deformation theory (FSDT), Matched asymptotic method (MAM) and multilayer method (MLM), for the purpose of elastic analysis of rotating thick truncated conical shells made of functionally graded materials (FGMs). Qinkai et al.[12] studied the effects of rotation upon frequency characteristics of rotating truncated conical shell and derived accurate expressions of centrifugal and coriolis accelerations and initial hoop tension and presented a modified dynamic model for the rotating truncated conical shell. Seidi et al. [13] presented an improved high-order theory for temperature-dependent buckling analysis of sandwich conical shell with thin functionally graded (FG) facesheets and homogenous soft core. Sofiyev [15] studied the buckling of freely-supported functionally graded (FG) truncated and complete conical shells under external pressures in the framework of the shear deformation theory (SDT). Sofiyev et al. [16] investigated the stability behavior of functionally graded (FG) truncated conical shell interacting with two-parameter elastic foundations within the shear deformation theory (SDT) according to the framework of the Donnell's shell theory. Zeighampour et al. [17] have developed the thin conical shell model by using the modified couple stress theory and derived the equations of motion with partial differentials and classical and non-classical boundary conditions by using Hamilton's principle.
Literature review, although points towards the popularity of the area of elastic analysis of FGM shells, however, to the best of the researcher's knowledge, no study has been carried out to date on FGM rotating conical shell modelled by Mori-Tanaka scheme, using elemental gradation of material properties. In the present study, rotating truncated conical shells, made up of axially varying FGM whose properties vary according to Mori-Tanaka scheme are analyzed using element based material gradation. The shells are subjected to variable internal pressure having clamped-clamped boundary condition. Aluminum as a metal and zirconia as ceramic is used and both metal-ceramic and ceramic-metal FGM shells are analyzed.

2 MATHEMATICAL FORMULATION

In shear deformation theory (SDT), the elements may have rotation, and the shear strain may not be zero means the straight lines perpendicular to the central axis of the truncated cone may rotate after loading and deformation (Nejad et al., [9]). Multilayer modeling is adopted for the shell geometry along with principle of stationary total potential for finite element formulation.

Fig.1 shows the geometric parameters for the modeling of axisymmetric cross section of the truncated conical shell. L and h are length and thickness and a and b are the inner radius at bottom and top surfaces of the shell. z is the distance of any point within the cross section from central plane, along the radial direction and x is height from the bottom edge, along axial direction. R is the distance of the central plane of the cross section, along the radial direction from the central axis of the shell, which is given by (Nejad *et al.*, [9]):

$$R = a + \frac{h}{2} - (\tan\beta)x \tag{1}$$

where β is half of the tapering angle, given as:

$$\beta = \tan^{-1}\left(\frac{a-b}{L}\right) \tag{2}$$

Young's modulus and density of the shell are assumed to vary according to the Mori-Tanaka scheme (Bayat et al., [2]) (Eqs. (3)-(9)). The effective bulk modulus and shear modulus of the FGM shell are given by:

$$B\left(x\right)=\left(B_o-B_i\right)/V_o\left(1+\left(1-V_o\right)\frac{3\left(B_o-B_i\right)}{3B_i+4G_i}\right)+B_i \tag{3}$$

$$G\left(x\right)=\left(G_o-G_i\right)/V_o\left(1+\left(1-V_o\right)\frac{\left(G_o-G_i\right)}{G_i+f_1}\right)+G_i \tag{4}$$

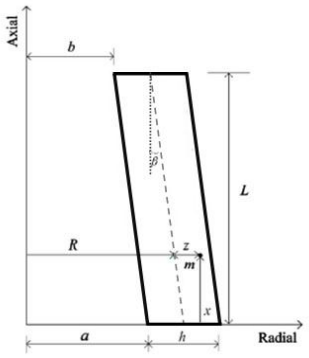

Fig.1
Geometric parameters of the shell.

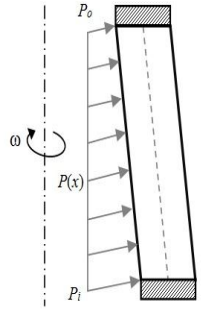

Fig.2
Boundary conditions applied.

$$f_1=\frac{G_i\left(9B_i+8G_i\right)}{6\left(B_i+2G_i\right)} \tag{5}$$

Here, V is the volume fraction of the phase material. The subscripts i and o refer to $x = 0$ and $x = L$ respectively. The volume fraction of the inner and outer phases are related by

$$V_i+V_o=1 \tag{6}$$

$$V_o=\left(\frac{x}{L}\right)^n \tag{7}$$

where n ($n \geq 0$) is the volume fraction exponent. The elastic modulus $E(x)$ can be found as:

$$E\left(x\right)=\frac{9B\left(x\right)G\left(x\right)}{3B\left(x\right)+G\left(x\right)} \tag{8}$$

The mass density ρ can be given by the rule of mixtures as:

$$\rho(x) = (\rho_o - \rho_i)\left(\frac{x}{L}\right)^n + \rho_i \tag{9}$$

In FEM, the functional grading is popularly carried out by assigning the average material properties over a given geometry followed by adhering the geometries thus resulting into layered functional grading of material properties. The downside of this approach is that it yields singular field variable values at the boundaries of the glued geometries, means a jump of the values of the material properties can be observed at the element boundaries. To get better results, instead of assigning average material properties to each element, material properties are varied inside the element boundaries, using same shape functions used to interpolate the displacement fields [18].

$$\phi^e = \sum_{i=1}^{8} \phi_i N_i \tag{10}$$

where ϕ^e is element material property, ϕ_i is material property at node *i* and N_i is the Shape function.

Fig. 2 shows the boundary conditions applied on the shells. Variable pressure field at the inner surface is given by (Nejad et al., [9]):

$$P(x) = P_i + (P_o - P_i)\left(\frac{x}{L}\right)^m \tag{11}$$

Axial component P_x and radial component P_z of $P(x)$ is given by

$$P_x = P\sin\beta \ , \ P_z = P\cos\beta \tag{12}$$

The rotating shell is modeled as a axisymmetric problem. Using linear quadrilateral element, the displacement vector $\{\varphi\}$ can be obtained as (Seshu [14]):

$$\{\varphi\} = \{u \quad v\}^T = [N]\{\delta\}^e \tag{13}$$

where *u* and *v* are the components of displacement in radial and axial direction respectively, $[N]$ is the matrix of linear shape functions and $\{\delta\}$ is the nodal displacement vector, given as:

$$[N] = \begin{bmatrix} N_1 & 0 & N_2 & 0 & N_3 & 0 & N_4 & 0 \\ 0 & N_1 & 0 & N_2 & 0 & N_3 & 0 & N_4 \end{bmatrix} \tag{14}$$

$$\{\delta\}^e = \{u_1 \quad v_1 \quad u_2 \quad v_2 \quad u_3 \quad v_3 \quad u_4 \quad v_4\}^T \tag{15}$$

By transforming the global co-ordinates into natural co-ordinates $(\xi - \eta)$, the shape functions are obtained as:

$$N_1 = \left(\frac{1}{4}\right)(1-\xi)(1-\eta) \tag{16}$$

$$N_2 = \left(\frac{1}{4}\right)(1+\xi)(1-\eta) \tag{17}$$

$$N_3 = \left(\frac{1}{4}\right)(1+\xi)(1+\eta) \tag{18}$$

$$N_4 = \left(\frac{1}{4}\right)(1-\xi)(1+\eta) \tag{19}$$

The strain components are related to elemental displacement components as:

$$\{\varepsilon\} = \{\varepsilon_r \quad \varepsilon_\theta \quad \varepsilon_z \quad \gamma_{rz}\}^T = \left\{\frac{\partial u}{\partial r} \quad \frac{u}{r} \quad \frac{\partial v}{\partial z} \quad \frac{\partial u}{\partial z} + \frac{\partial v}{\partial r}\right\}^T \tag{20}$$

$$\left\{\frac{\partial u}{\partial r} \quad \frac{u}{r} \quad \frac{\partial v}{\partial z} \quad \frac{\partial u}{\partial z} + \frac{\partial v}{\partial r}\right\}^T = [B_1] \times \left\{\frac{\partial u}{\partial r} \quad \frac{\partial u}{\partial z} \quad \frac{\partial v}{\partial r} \quad \frac{\partial v}{\partial z} \quad \frac{u}{r}\right\}^T \tag{21}$$

where $\varepsilon_r, \varepsilon_\theta, \varepsilon_z$ and γ_{rz} are radial, tangential, axial and shear strain respectively. By transforming the global co-ordinates into natural co-ordinates $(\xi - \eta)$,

$$\left\{\frac{\partial u}{\partial r} \quad \frac{\partial u}{\partial z} \quad \frac{\partial v}{\partial r} \quad \frac{\partial v}{\partial z} \quad \frac{u}{r}\right\}^T = [B_2] \times \left\{\frac{\partial u}{\partial \xi} \quad \frac{\partial u}{\partial \eta} \quad \frac{\partial v}{\partial \xi} \quad \frac{\partial v}{\partial \eta} \quad \frac{u}{r}\right\}^T \tag{22}$$

$$\left\{\frac{\partial u}{\partial \xi} \quad \frac{\partial u}{\partial \eta} \quad \frac{\partial v}{\partial \xi} \quad \frac{\partial v}{\partial \eta} \quad \frac{u}{r}\right\}^T = [B_3] \times \{\delta\}^e \tag{23}$$

The above elemental strain-displacement relationships can be written as:

$$\{\varepsilon\} = [B]\{\delta\}^e \tag{24}$$

where $[B]$ is strain-displacement relationship matrix, which contains derivatives of shape functions. For a linear quadrilateral element it is calculated as:

$$[B] = [B_1] \times [B_2] \times [B_3] \tag{25}$$

$$[B_1] = \begin{bmatrix} 1 & 0 & 0 & 0 & 0 \\ 0 & 0 & 0 & 0 & 1 \\ 0 & 0 & 0 & 1 & 0 \\ 0 & 1 & 1 & 0 & 0 \end{bmatrix} \tag{26}$$

$$[B_2] = \begin{bmatrix} \frac{J_{22}}{|J|} & \frac{-J_{12}}{|J|} & 0 & 0 & 0 \\ \frac{-J_{21}}{|J|} & \frac{J_{11}}{|J|} & 0 & 0 & 0 \\ 0 & 0 & \frac{J_{22}}{|J|} & \frac{-J_{12}}{|J|} & 0 \\ 0 & 0 & \frac{-J_{21}}{|J|} & \frac{J_{11}}{|J|} & 0 \\ 0 & 0 & 0 & 0 & 1 \end{bmatrix} \tag{27}$$

where J is the Jacobian matrix, used to transform the global co-ordinates into natural co-ordinates. It is given as:

$$[J]=\begin{bmatrix}\sum_{i=1}^{4}\frac{\partial N_i}{\partial \xi}r_i & \sum_{i=1}^{4}\frac{\partial N_i}{\partial \xi}z_i \\ \sum_{i=1}^{4}\frac{\partial N_i}{\partial \eta}r_i & \sum_{i=1}^{4}\frac{\partial N_i}{\partial \eta}z_i\end{bmatrix} \tag{28}$$

$$[B_3]=\begin{bmatrix}\frac{\partial N_1}{\partial \xi} & 0 & \frac{\partial N_2}{\partial \xi} & 0 & \frac{\partial N_3}{\partial \xi} & 0 & \frac{\partial N_4}{\partial \xi} & 0 \\ \frac{\partial N_1}{\partial \eta} & 0 & \frac{\partial N_2}{\partial \eta} & 0 & \frac{\partial N_3}{\partial \eta} & 0 & \frac{\partial N_4}{\partial \eta} & 0 \\ 0 & \frac{\partial N_1}{\partial \xi} & 0 & \frac{\partial N_2}{\partial \xi} & 0 & \frac{\partial N_3}{\partial \xi} & 0 & \frac{\partial N_4}{\partial \xi} \\ 0 & \frac{\partial N_1}{\partial \eta} & 0 & \frac{\partial N_2}{\partial \eta} & 0 & \frac{\partial N_3}{\partial \eta} & 0 & \frac{\partial N_4}{\partial \eta} \\ \frac{N_1}{r} & 0 & \frac{N_2}{r} & 0 & \frac{N_3}{r} & 0 & \frac{N_4}{r} & 0\end{bmatrix} \tag{29}$$

From generalized hooks law, components of stresses in radial, circumferential and axial direction ($\sigma_r,\sigma_\theta,\sigma_z$ and τ_{rz}) are related to components of total strain as:

$$\varepsilon_r=\frac{1}{E}\left(\sigma_r-\nu\sigma_\theta-\nu\sigma_z\right) \tag{30}$$

$$\varepsilon_\theta=\frac{1}{E}\left(\sigma_\theta-\nu\sigma_r-\nu\sigma_z\right) \tag{31}$$

$$\varepsilon_z=\frac{1}{E}\left(\sigma_z-\nu\sigma_\theta-\nu\sigma_r\right) \tag{32}$$

In generalized matrix notation, stress-strain relation can be written as:

$$\{\sigma\}=\left[D\left(x\right)\right]\{\varepsilon\} \tag{33}$$

where $D\left(x\right)$ is stress-strain relationship matrix and is a function of x.

$$\{\sigma\}=\{\sigma_r \quad \sigma_\theta \quad \sigma_z \quad \tau_{rz}\}^T \tag{34}$$

$$D\left(x\right)=\frac{\left(1-\nu\right)E\left(x\right)}{\left(1+\nu\right)\left(1-2\nu\right)}\begin{bmatrix}1 & \frac{\nu}{\left(1-\nu\right)} & \frac{\nu}{\left(1-\nu\right)} & 0 \\ \frac{\nu}{\left(1-\nu\right)} & 1 & \frac{\nu}{\left(1-\nu\right)} & 0 \\ \frac{\nu}{\left(1-\nu\right)} & \frac{\nu}{\left(1-\nu\right)} & 1 & 0 \\ 0 & 0 & 0 & \frac{1-2\nu}{2\left(1-\nu\right)}\end{bmatrix} \tag{35}$$

$$\{\varepsilon\} = \{\varepsilon_r \quad \varepsilon_\theta \quad \varepsilon_z \quad \gamma_{rz}\}^T \tag{36}$$

when the shell rotates and is subjected to internal pressure, it experiences a distributed force over its volume and surface. Under these forces when shell is properly supported (so as to prevent rigid body motion), it undergoes deformation and stores internal strain energy U, which is given by:

$$U = \frac{1}{2}\int_V \{\varepsilon\}^T \{\sigma\}\, dv \tag{37}$$

Also the potential of external body and surface force is given by

$$V = -\int_V \{\delta\}^T \{q_v\} dv - \int_S \{\delta\}^T \{q_s\} ds \tag{38}$$

The element level equation can be written as:

$$U^e = \int_V \frac{1}{2}\{\delta\}^{eT} [B]^T [D(x)][B]\{\delta\}^e \, dv \tag{39}$$

$$V^e = -\int_V \{\delta\}^{eT} [N]^T \{q_v\} dv - \int_S \{\delta\}^{eT} [N]^T \{q_s\} ds \tag{40}$$

The total potential of the element can be written as:

$$\pi_p{}^e = \int_V \frac{1}{2}\{\delta\}^{eT} [B]^T [D(x)][B]\{\delta\}^e \, dv - \int_V \{\delta\}^{eT} [N]^T \{q_v\} dv - \int_S \{\delta\}^{eT} [N]^T \{q_s\} ds \tag{41}$$

Defining element stiffness matrix $[K]^e$ and element load vector $\{f\}^e$ as:

$$[K]^e = \int_V [B]^T [D(x)][B]\, dv \tag{42}$$

$$\{f\}^e = \int_V \{\delta\}^{eT} [N]^T \{q_v\} dv + \int_S \{\delta\}^{eT} [N]^T \{q_s\} ds \tag{43}$$

Taking axisymmetric element, thickness of the element will be $2\pi(R+z)$, therefore:

$$[K]^e = 2\pi \iint [B]^T [D(x)][B] (R+z) dr dz \tag{44}$$

$$\{f\}^e = 2\pi \int_V \{\delta\}^{eT} [N]^T \{q_v\} (R+z) dr dz + \int_S \{\delta\}^{eT} [N]^T \{q_s\} dr dz \tag{45}$$

Transforming global co-ordinates into natural co-ordinates

$$[K]^e = 2\pi \int_{-1}^{1}\int_{-1}^{1} [B]^T [D(x)][B] (R+z) |J| d\xi d\eta \tag{46}$$

$$\{f\}^e = 2\pi \int_V \{\delta\}^{eT} [N]^T \{q_v\}(R+z)|J|d\xi d\eta + \int_S \{\delta\}^{eT} [N]^T \{q_s\}|J|d\xi d\eta \tag{47}$$

Total potential energy of the shell is given by

$$\pi_p = \sum \pi_p^e \tag{48}$$

Using the Principle of stationary total potential (PSTP) the total potential is set to be stationary with respect to small variation in the nodal degree of freedom that is:

$$\frac{\partial \pi_p}{\partial \{\delta\}^T} = 0 \tag{49}$$

which gives system level equation for shell as:

$$[K]\{\delta\} = \{F\} \tag{50}$$

where

$$[K] = \sum_{n=1}^{N} [K]^e = Globel\ Stiffness\ matrix \tag{51}$$

$$\{F\} = \sum_{n=1}^{N} [f]^e = Globel\ load\ vector \tag{52}$$

3 RESULTS

3.1 Validation of the work

To validate the current work, a similar problem of conical Shell, previously analyzed is reconsidered. The shell has geometric parameters as (Nejad et al., [9]): $L = 400mm, h = 20mm, a = 40mm$ and $b = 30mm$. Material gradation is done by power law, and shell has clamped-clamped boundary condition. Circumferential stresses for $\omega = 0,1000$ and 2000 *rad/s* are evaluated taking $m = n = 1$ and a comparison with reference is presented in Fig 3. Both the results are in good agreement.

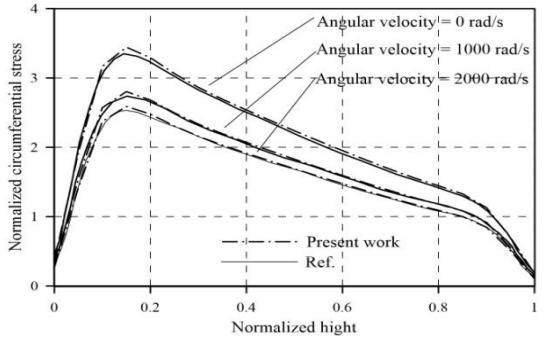

Fig.3
Validation of the work.

3.2 Numerical results

In this section a conical FGM shell is analyzed. Aluminum as metal and zirconia as ceramic is taken and Ceramic-metal and Metal-ceramic both the FGM are considered. The Young's modulus (E), density (ρ), bulk modulus (B),

shear modulus (G) and Poisson's ratio (υ) of aluminum and zirconia are given as (Bayat et al., [2]): $E_{Al} = 70GPa$, $E_{cer} = 151GPa, \rho_{Al} = 2700kg/m^3, \rho_{cer} = 5700kg/m^3, B_{Al} = 58.3333GPa, B_{cer} = 128.8333GPa, G_{Al} = 26.9231GPa$, $G_{cer} = 58.0769GPa, \upsilon = 0.3$. The shell has geometric parameters as $L = 400mm, h = 20mm, a = 40mm$ and $b = 30mm$. Shell has clamped-clamped boundary condition and P_i and P_0 are taken as 120 *MPa* and 40 *MPa*. Stress and deformation is presented in non dimensional form. To normalize stress, it is divided by average pressure and to normalize displacement, it is divided by inner radius *a*.

$$\bar{\sigma} = \frac{\sigma}{\bar{P}} \qquad \bar{P} = \frac{P_i + P_o}{2} \qquad \bar{u} = \frac{u}{a} \times 1000 \tag{53}$$

where

$$\bar{\sigma} = Normalized\ Stress, \bar{P} = Average\ \text{Pr}essure, \bar{u} = Normalized\ Displacement$$

Fig 4. to Fig 7. shows the distributions of normalized radial displacement, radial stress, circumferential stress and shear stress respectively. All the distributions are along the axial direction and evaluated at 2000 *rad/s*, for metal-ceramic FGM shells. Pressure grading and material grading both the parameters are taken as 1 i.e. $m = n = 1$.

It is observed that deformation in radial direction is minimum that is zero, at bottom and top surface, which confirms the clamped-clamped boundary condition applied to the shell. Deformations are maximum at the inner layer i.e. at $z = -h/2$, near the bottom surfae and decreases gradually till the outer layer ($z = h/2$), top surface. Radial stresses are tensile and compressive both in nature. Compressive radial stress is more as compared to tensile radial stress. Tensile radial stress occurs only in a small zone near top and bottom surface and rest of the intermediate height zone has compressive radial stress. Circumferential stresses are only tensile. It is maximum at the inner layer, near the bottom surface, and decreases gradually upto the top surface and outer layer. Shear stress varies only in a small zone near the top and bottom surface and remains same in all the layers at intermediate heights. It is maximum at the bottom surface (at $x = 0$) and inner layer (at $z = -h/2$).

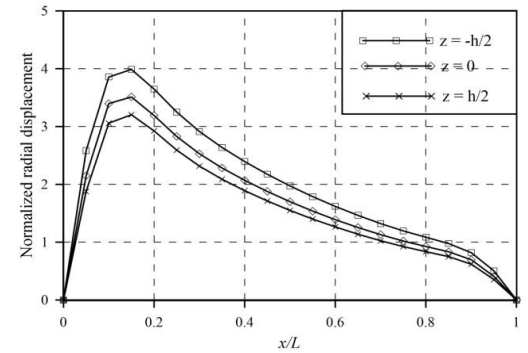

Fig.4
Normalized radial displacement ($m = 1, n = 1, \omega = 2000$).

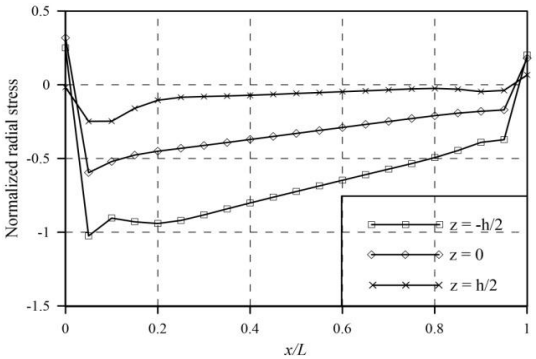

Fig.5
Normalized radial stress ($m = 1, n = 1, \omega = 2000$).

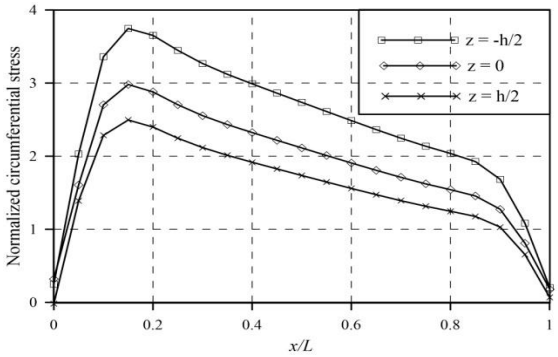

Fig.6
Normalized circumferential stress ($m=1, n=1, \omega=2000$).

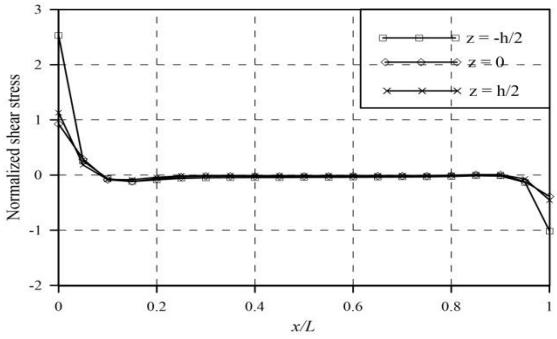

Fig.7
Normalized shear stress ($m=1, n=1, \omega=2000$).

It can be seen from Fig 8. and Fig 9. that there is a significant increase in deformation and stress as pressure gradient index *m* increases upto 1.5 and above 1.5 there is a slight increase in deformation and stress.

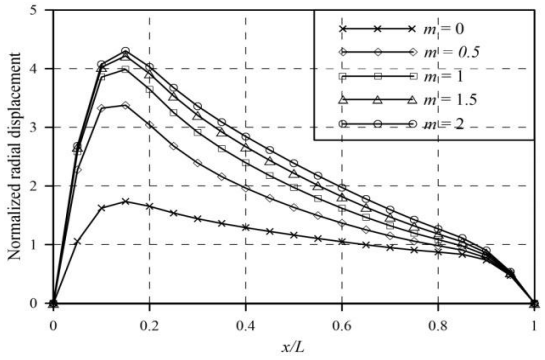

Fig.8
Normalized radial displacement ($n=1, z=-h/2, \omega=2000$).

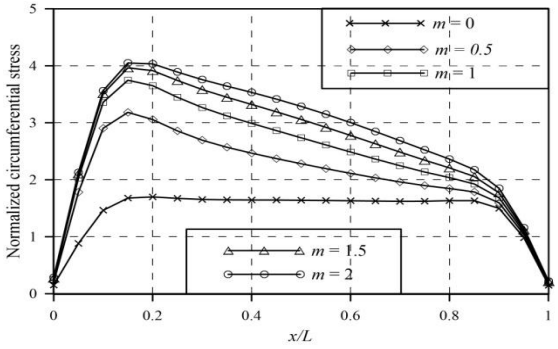

Fig.9
Normalized circumferential stress ($n=1, z=-h/2, \omega=2000$).

Fig 10. to Fig 13. shows the distribution of radial displacement and circumferential stress for different material grading index *n* in ceramic-metal and metal-ceramic FGM respectively. It can be seen that in ceramic-metal FGM shell deformation is maximum and stress is minimum for $n=0$, which is completely metallic shell. Deformation decreases and stress increases with increasing *n*. In metal-ceramic shell deformation is maximum and stress is minimum for $n=0$ that is completely ceramic shell, and deformation increases and stress decreases with increasing *n*. By comparing both metal-ceramic and ceramic-metal FGM shells (Fig 14. and Fig 15.), it is observed that complete ceramic shell has lowest deformation and highest stress while complete metallic shell has highest deformation and lowest stress. Both material are not economical as compared to FGMs. Because ceramic has high density, therefore complete ceramic shell will be of highest weight and complete metallic shell has very high deformation. Therefore to optimize weight to strength and deformation to strength ratio according to requirement (allowable deformation or allowable stress), using FGM, having grading index 2 is more economical than homogeneous shells.

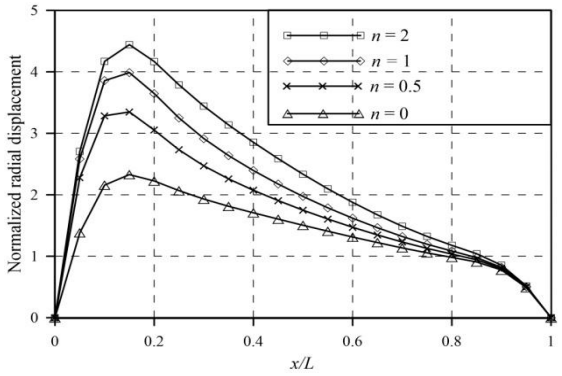

Fig.10
Normalized radial displacement, ceramic-metal shell ($m=1$, ($z=-h/2, \omega=2000$).

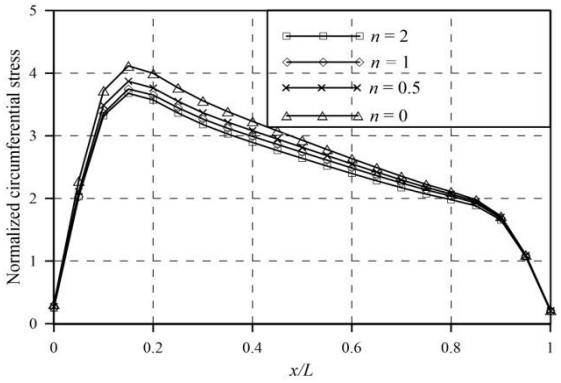

Fig.11
Normalized circumferential stress, ceramic-metal shell ($m=1$, ($z=-h/2, \omega=2000$).

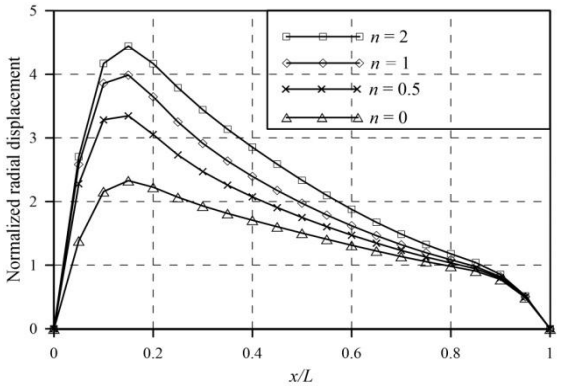

Fig.12
Normalized radial displacement, metal-ceramic shell ($m=1$, ($z=-h/2, \omega=2000$).

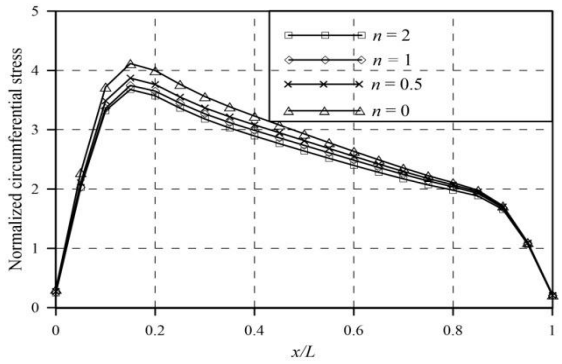

Fig.13
Normalized circumferential stress, metal- ceramic shell $m=1,\ z=-h/2,\omega=2000$).

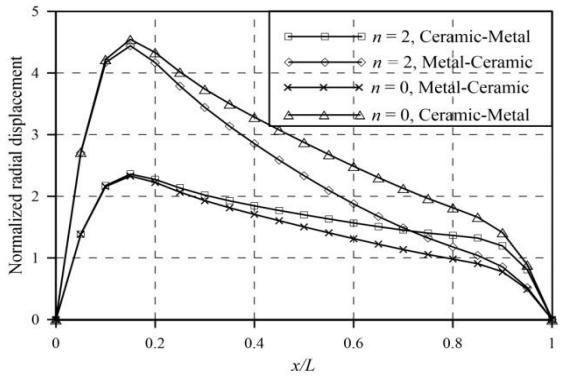

Fig.14
Comparison of Normalized radial displacement ($m=1,$ ($z=-h/2,\omega=2000$).

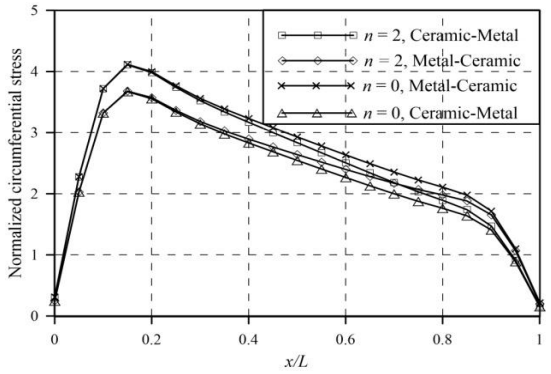

Fig.15
Comparison of Normalized circumferential stress ($m=1,$ ($z=-h/2,\omega=2000$).

4 CONCLUSIONS

In the present study stress and deformation analysis of rotating thick truncated conical shells made up of functionally graded material is done. Material properties are modeled by Mori-Tanaka scheme, which is achieved by element based material grading. The shells are subjected to clamped-clamped boundary condition and variable internal pressure. Shear deformation theory and multilayer modeling is used and the governing equations are modeled using principle of stationary total potential. The element based grading of material property yields an appropriate approach of functional grading as the shape functions in the elemental formulations being coordinate functions make it easier to implement the same. Layered functional grading over discrete area instead of elements, offer singularities in the field variables at adjoining lines or surfaces. Numerical results are obtained for metal-ceramic and ceramic-metal FGM of aluminum and zirconia. On the basis of results obtained it can be concluded that deformation and stresses are more in the inner layer, near the bottom surface and increases with increasing pressure gradient *m*. Further to

optimize weight to strength and deformation to strength ratio according to requirement (allowable deformation or allowable stress), using FGM having grading index 2 is more suitable than homogeneous shells.

REFERENCES

[1] Asemi K., Akhlaghi M., Salehi M., Zad S.K.H., 2011, Analysis of functionally graded thick truncated cone with finite length under hydrostatic internal pressure, *Archive of Applied Mechanics* **81**: 1063-1074.

[2] Bayat M., Sahari B., Saleem M., Dezvareh S., Mohazzab A.H., 2011, Analysis of functionally graded rotating disks with parabolic concave thickness applying an exponential function and the mori-tanaka scheme, *IOP Conference Series: Materials Science and Engineering* **17**: 1-11.

[3] Civalek O., 2006, The determination of frequencies of laminated conical shells via the discrete singular convolution method, *Journal of Mechanics of Materials and Structures* **1**: 163-182.

[4] Civalek O., Gürses M., 2009, Free vibration analysis of rotating cylindrical shells using discrete singular convolution technique, *International Journal of Pressure Vessels and Piping* **86**: 677-683.

[5] Heydarpour Y., Aghdam M.M., 2016, Transient analysis of rotating functionally graded truncated conical shells based on the Lord–Shulman model, *Thin-Walled Structures* **104**: 168-184.

[6] Hua L., 2000, Frequency analysis of rotating truncated circular orthotropic conical shells with different boundary conditions, *Composites Science and Technology* **60**: 2945-2955.

[7] Ma X., Jin G., Xiong Y., Liu Z., 2014, Free and forced vibration analysis of coupled conical–cylindrical shells with arbitrary boundary conditions, *International Journal of Mechanical Sciences* **88**: 122-137.

[8] Malekzadeh P., Daraie M., 2014, Dynamic analysis of functionally graded truncated conical shells subjected to asymmetric moving loads, *Thin-Walled Structures* **84**:1-13.

[9] Nejad M.Z., Jabbari M., Ghannad M., 2015, Elastic analysis of FGM rotating thick truncated conical shells with axially-varying properties under non-uniform pressure loading, *Composite Structures* **122**: 561-569.

[10] Nejad M.Z., Jabbari M., Ghannad M., 2014, Elastic analysis of rotating thick truncated conical shells subjected to uniform pressure using disk form multilayers, *ISRN Mechanical Engineering* **2014**: 1-10.

[11] Nejad M.Z., Jabbari M., Ghannad M., 2014, A semi analytical solution of thick truncated cones using matched asymptotic method and disk form multilayers, *Archive of Mechanical Engginering* **61**: 495-513.

[12] Qinkai H., Fulei C., 2013, Effect of rotation on frequency characteristics of a truncated circular conical Shell, *Archive of Applied Mechanics* **83**: 1789-1800.

[13] Seidi J., Khalili S.M.R., Malekzadeh K., 2015, Temperature-dependent buckling analysis of sandwich truncated conical shells with FG facesheets, *Composite Structures* **131**: 682-691.

[14] Seshu P., 2003, *A Text Book of Finite Element Analysis*, PHI Learning Pvt, Ltd.

[15] Sofiyev A.H., 2015, Buckling analysis of freely-supported functionally graded truncated conical shells under external pressures, *Composite Structures* **132**: 746-758.

[16] Sofiyev A.H., Kuruoglu N., 2016, Combined effects of elastic foundations and shear stresses on the stability behavior of functionally graded truncated conical shells subjected to uniform external pressures, *Thin-Walled Structures* **102**: 68-79.

[17] Zeighampour H., Beni Y.T., 2014, Analysis of conical shells in the framework of coupled stresses theory, *International Journal of Engineering Science* **81**: 107-122.

[18] Thawait A. K., Sondhi L., Bhowmick S., Sanyal S., 2017, An investigation of stresses and deformation states of clamped rotating functionally graded disks, *Journal of Theoretical and Applied Mechanics* **55**: 189-198.